Anomalous X-ray Study on the Defect Structure of Nano-ITO

G. B. González,[1] J. P. Quintana,[1] T. O. Mason,[1] J.P. Hodges,[2] J.D. Jorgensen[2]
[1]Northwestern University, Evanston, IL, U.S.A.
[2]Argonne National Laboratory, Argonne, IL, U.S.A.

Introduction

Sn-doped In_2O_3 is an n-type transparent conducting oxide (TCO) with extensive commercial applications, including flat-panel displays, solar cells, and energy efficient windows [1]. Although indium tin oxide (ITO) is a widely used TCO, knowledge about its defect structure is limited.

ITO and In_2O_3 crystallize in the cubic bixbyite or C-type rare-earth sesquioxide structure, Ia3 space group (number 206). The bixbyite structure is similar to the fluorite structure, but one-fourth of the anions are vacant, allowing for small shifts of the ions [2]. In_2O_3 has two nonequivalent sixfold coordinated cation sites. Figure 1 shows the two cation sites, which are referred to as equipoints "b" and "d" [3]. The b site cations have six equidistant oxygen anion neighbors at 2.18 Å that lie approximately at the corners of a cube with two anion structural vacancies along one body diagonal [4]. The d site cations are coordinated to six oxygen anions at three different distances: 2.13, 2.19, and 2.23 Å. These oxygen anions are near the corners of a distorted cube, with two empty anions along one face diagonal.

ITO exhibits higher conductivities and carrier concentrations than pure In_2O_3 because of the electron compensation of the $Sn^{\bullet}$ species. An existing model of the defect chemistry of ITO has been inferred from measured electrical properties of the material [5], following the anion interstitial model for doped In_2O_3 structures [2, 6]. The model consists of completely filled cation sites, and an excess of $\delta/2$ O_i'' anions fill some of the structural anion vacancy sites of In_2O_3. The interstitial anions compensate the charge of the δ ionized tin donors [given the charge of the $(Sn^{4+})^{\bullet}_{In3+}$ species], which go into the indium sites. When Kröger-Vink notation is used, the material is formally described as $In_{2-\delta}\ Sn_{\delta}^{\bullet}\ (O_i'')_{\delta/2}\ O_3$.

Frank and Köstlin [5] also proposed the existence of defect associates whose concentrations depend on oxygen partial pressure and tin content. At high oxygen partial pressure and medium tin doping levels, the proposed defects are mainly $(2Sn_{In}^{\bullet}O_i'')^x$ and $(2Sn_{In}^{\bullet}3O_OO_i'')^x$. The $(2Sn_{In}^{\bullet}O_i'')^x$ associate, formed by two nonadjacent Sn^{4+} ions and an oxygen interstitial anion, is a loosely bound cluster that decomposes upon reduction as follows: $(2Sn_{In}^{\bullet}O_i'')^x \rightarrow \frac{1}{2}O_2(g) + 2\ Sn_{In}^{\bullet} + 2\ e'$.

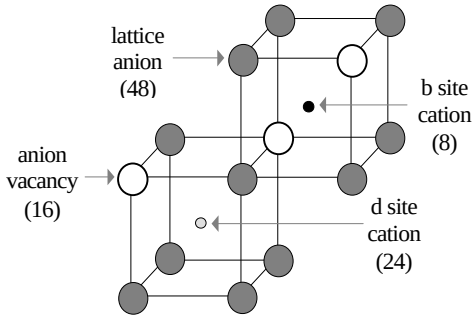

FIG. 1. Nonequivalent cation sites in ITO.

The electrons that charge-compensate the $Sn_{In}^{\bullet}$ species increase the conductivity in reduced ITO samples. On the other hand, the nonreducible defect $(2Sn_{In}^{\bullet}3O_OO_i'')^x$ is a tightly bound cluster formed by two Sn^{4+} cations on nearest neighbor sites, three lattice oxygen ions, and one oxygen interstitial anion. This defect exists even under reducing conditions and ties in the $Sn_{In}^{\bullet}$ species, resulting in an unchanged conductivity even when more Sn dopant is added to the structure.

To study the defect structure of ITO, the cation distribution and the presence of oxygens at the anion structural vacancies are extremely important. Given the proximity of In and Sn in the periodic table, their x-ray scattering factors are similar. In order to distinguish them, x-ray energies near the absorption edges were used to maximize their contrast. Structural information on oxygen and accurate Debye-Waller factors were obtained from time-of-flight (TOF) neutron diffraction experiments. The synchrotron and neutron diffraction data were combined to fully investigate the defect structure.

Methods and Materials

The starting materials were In_2O_3, 99.99% (Aldrich Chemical Co., Milwaukee, WI) and commercially prepared nanocrystalline 9 cation % ITO powders (Nanophase Technologies, Burr Ridge, IL). Pellets of nano-ITO were pressed and presintered at 700°C for 1 h. Nano-ITO pellets were cut into rectangular bars (approximately $2 \times 3 \times 8$ mm) from the pellets by using a diamond saw. Two pure In_2O_3 were pressed and sintered at 1350°C in high-density alumina crucibles.

One In_2O_3 and one nano-ITO sample were reduced in H_2/N_2 gas for 8 h at 500ºC. The other pure In_2O_3 and ITO samples were annealed in air for 8 h at 500ºC. All samples were quenched in air to room temperature.

Simultaneous conductivity and thermopower measurements were made by using a PC-controlled system including a scanner, current source, and digital multimeter (Models 705, 224, and 196, respectively, Keithley Instruments, Inc., Cleveland, OH). Four S-type thermocouples (Pt/Pt-10% Rh) were employed by using the steady-state gradient technique [7]. A current-reversal technique was employed to correct conductivity voltages for thermal emf. The thermal gradients employed were typically 15-20K over the 8-mm length of the samples measured. Thermoelectric coefficients were corrected for the thermopower of platinum.

TOF neutron powder diffraction data were collected on the powder samples at room temperature by using the special environment powder diffractometer (SEPD) at the Intense Pulsed Neutron Source (IPNS) [8] at Argonne National Laboratory. Diffraction data were collected from the high-resolution back-scattering detectors ($\Delta d/d$ = 0.0035). Because the absorption cross section of indium is significantly large (σ_a = 194 barns for λ = 1.8 Å), an incident spectrum was collected downstream from the In_2O_3 powder sample. This incident spectrum was used to normalize diffraction data collected for all samples, thus providing a correction for the sample absorption.

Synchrotron high-resolution powder diffraction data were collected on the nano-ITO samples at the 5-BM-C beam station at the DuPont-Northwestern-Dow Collaborative Access Team (DND-CAT) sector. The 5-BM-C beam station has a two-circle diffractometer with a Ge(220) crystal analyzer and vertical Soller slits, resulting in high-resolution diffraction data (full width at half maximum [FWHM] of ~0.05º for nano-ITO, and FWHM of ~0.005º for bulk powders). Diffraction patterns were collected at the In K edge (27,940 eV) and 100 eV below it (27,840 eV) to maximize the contrast of the In and Sn cations. Samples in glass capillary tubes were run in transmission mode. The experimental anomalous f ' and f " scattering correction terms at the two energies were obtained by analyzing x-ray fine structure (XAFS) scans of the samples with the program Chooch [9]. The two x-ray patterns combined with the TOF neutron diffraction data were refined with the Rietveld method [10] by using the FullProf program [11].

Results

The conductivity for the oxidized nano-ITO was $25(\Omega cm)^{-1}$. For the H_2/N_2 reduced nano-ITO sample (p_{O2} of ~10^{-5} atm), it increased to $95(\Omega cm)^{-1}$. The corresponding thermopowers were –115 µV/K and -90 µV/K. The conductivity and thermopower were measured *in-situ* at 500ºC.

Table 1 summarizes the results obtained from Rietveld analysis of x-ray and neutron diffraction data. The reduced In_2O_3 data are not shown, since they gave the same diffraction results (within experimental errors) as the oxidized In_2O_3.

Table 1. Structural results obtained from Rietveld refinement of combined x-ray and neutron data.

	In_2O_3	ITO air	ITO H_2/N_2
Cation b (x = y = z = ¼)			
B (Å)	0.441(55)	0.606(52)	0.453(43)
Sn/In + Sn		0.239(44)	0.146(37)
Cation d (y = 0, z = ¼)			
B (Å)	0.337(32)	0.358(23)	0.383(21)
x	0.4662(1)	0.4688(1)	0.4680(1)
Sn/In + Sn		0.039(15)	0.070(12)
O_s (structural oxygen)			
B (Å)	0.533(26)	0.616(18)	0.567(22)
x	0.3904(1)	0.3896(2)	0.3901(1)
y	0.1549(1)	0.1539(1)	0.1541(1)
z	0.3819(1)	0.3818(1)	0.3817(1)
O_i (interstitial oxygen)			
x	0.088	0.094(1)	0.088(2)
O_i fraction	-0.008(5)	0.105(8)	0.060(7)
Total Sn %		8.9	9.0
Sn/O_i		1.8(1)	3.0(3)
a (Å)	10.1216(1)	10.1250(2)	10.1336(5)
Refinement parameters			
$R_{Bragg\text{-}x\text{-}ray}$		2.76	2.28
$R_{Bragg\text{-}x\text{-}ray}$		4.99	4.19
$R_{Bragg\text{-}neutron}$	4.00	2.51	2.07
χ^2	1.43	1.53	1.58

Discussion

The conductivity and thermopower results are consistent with n-type behavior and with carrier contents increasing with reduction. The Rietveld results for the oxidized nano-ITO sample agree with Mössbauer results [12, 13] and recent full-potential linear muffin-tin orbital (FLMTO) electronic calculations [14], which show a strong preference of tin for occupying the b site rather than the d site. However, for the reduced nano-ITO sample, the preference is not as strong. Another observation is that interstitial oxygen anions are absent in the pure In_2O_3 samples and present in both ITO samples.

The ratio of tin to interstitial oxygen of 1.8:1 in the oxidized sample supports the existence of $(2Sn_{In}^{\bullet}O_i'')^x$ and $(2Sn_{In}^{\bullet}3O_OO_i'')^x$ defects postulated by Frank and Köstlin. Both defects are believed to have two tin cations and one oxygen interstitial anion (2:1 tin-to-interstitial ratio).

Upon a decrease in the oxygen partial pressure, the reducible defects, having non-nearest-neighbor Sn ions, get ionized, thereby freeing up the $Sn_{In}^{\bullet}$ donors, which contribute to an increase in conductivity. Furthermore, the tin-to-interstitial oxygen ratio would be expected to increase (observed ratio is 3.0:3) but not go to infinity because of the presence of $(2Sn_{In}^{\bullet}3O_OO_i'')^x$ defects. As mentioned before, the nonreducible defect species proposed by Frank and Köstlin involves two adjacent tin cations, one interstitial oxygen anion, and three lattice oxygen anions. Because of the proximity of the tin cations to the oxygen anions, this cluster is not readily reduced. This means that such tin ions contribute to the measured Sn concentrations but do not affect the carrier concentrations. Therefore, any interstitial oxygen anions that participate in the nonreducible defects remain present, even at low oxygen partial pressures, as observed for the reduced ITO samples.

Increases in the lattice parameter with Sn doping and with decreasing oxygen partial pressure have been reported before [1, 5, 13]. These trends were also observed in the present study. The increase in the lattice parameter with increasing Sn concentration is attributed to the increase in the repulsive forces arising from the extra positive charge of the $Sn^{\bullet}$ cations. In the oxidized state, the interstitial oxygen anions charge-compensate the material. However, as those interstitial oxygen anions are removed during reduction, the repulsive forces increase, leading to an enlargement of the unit cell. Therefore, the reduced ITO exhibits a lattice constant greater than that of the oxidized ITO.

Acknowledgments

This research was sponsored by the U.S. Department of Energy (DOE) under Grant No. DE-FG02-84ER45097. The use of the APS was supported by the DOE Office of Science, Office of Basic Energy Sciences, under Contract No. W-31-109-ENG-38. DND-CAT is supported through E. I. duPont de Nemours & Co., Northwestern University, The Dow Chemical Co., the State of Illinois through the U.S. Department of Commerce and the Illinois Board of Higher Education-Higher Education Cooperation Act (IBHE-HECA), the DOE Office of Energy Research, and the U.S. National Science Foundation, Division of Materials Research.

References

[1] J. C. C. Fan and F. J. Bachner, J. Electrochem. Soc. **122**, 1719 (1975).
[2] J. H. W. De Witt, J. Solid State Chem. **20**, 143 (1977).
[3] A. J. C. Wilson (editor), *The International Union of Crystallography, International Tables for Crystallography* (Kluwer Academic Publishers, Dordrecht, The Netherlands, 1992).
[4] M. Marezio, Acta Crystallogr. **20**, 723 (1966).
[5] G. Frank and H. Köstlin, Appl. Phys. A **27**, 197 (1982).
[6] E. C. Subbarao, P. H. Sutter, and J. Hrizo, J. Am. Ceram. Soc. **48**, 443 (1965).
[7] A. Trestman-Matts, S. Dorris, and T. O. Mason, J. Am. Ceram. Soc. **66**, 589 (1983).
[8] J. D. Jorgensen, J. Faber, J. M. Carpenter, R. K. Crawford, J. R. Haumann, R. L. Hitterman, R. Kleb, G. E. Ostrowski, F. J. Rotella, and T. G. Worlton, J. Appl. Cryst. **22**, 321 (1989).
[9] G. Evans and R. F. Pettifer, J. Appl. Crystallogr. **34**, 82 (2001).
[10] H. Rietveld, J. Appl. Crystallogr. **2**, 65 (1969).
[11] J. Rodríguez-Carvajal, *Reference Guide for the Computer Program FullProf* (Laboratoire Leon Brilloui, CEA-CNRS, Saclay, France, 1997).
[12] K. Nomura, Y. Ujihira, S. Tanaka, and K. Matsumoto, Hyperfine Interact. **42**, 1207 (1988).
[13] N. Nadaud, N. Lequeux, M. Nanot, J. Jové, and T. Roisnel, J. Solid State Chem. **135**, 140 (1998).
[14] O. N. Mryasov and A. J. Freeman, Phys. Rev. B **64**(23), art. no. 233111 (2001).